

RESEARCH BULLETIN 851

FEBRUARY 1964

UNIVERSITY OF MISSOURI COLLEGE OF AGRICULTURE  
AGRICULTURAL EXPERIMENT STATION

# A Hydrodynamic Analog Study of Grain Aeration Cooling

GARY A. HOHNER AND D. B. BROOKER



(Publication Authorized February 14, 1964)

COLUMBIA, MISSOURI

---

## CONTENTS

Introduction .....	3
Definition of Symbols .....	4
Previous Approaches to Porous Media Problems .....	5
Equipment .....	7
Test Procedure .....	9
Validity of the Analog .....	12
Scaling the Analog System .....	12
Discussion of Results .....	14
Conclusions .....	25
Bibliography .....	26
Appendix .....	27
Derivation of the Laplacian Field Equation from the Navier-Stokes Fluid Flow Equation .....	27
Derivation of the Resistance to Fluid Flow in a Laplacian Field in the Fluid Mapper .....	29

This bulletin is a report on Department  
of Agricultural Engineering research  
project 225, Grain Drying

# A Hydrodynamic Analog Study of Grain Aeration Cooling

GARY A. HOHNER AND D. B. BROOKER

Interest in the in-storage aeration cooling of grain has grown out of need for a cheap and efficient method of reducing and equalizing grain temperature, preventing moisture migration and providing a vehicle for grain fumigation. Long storage periods and increased stores of grain have made "turning" the grain more costly and time-consuming.

Various methods of in-storage grain aeration have been devised. One of the common systems used in the upright cylindrical grain storage tanks of large commercial grain establishments is called the cross-flow aeration system (1). This system consists of a pair of perforated air ducts located opposite each other and extending vertically up the inside walls of the cylindrical tank. Each duct is semi-circular in shape with one acting as the inlet duct and one as the exhaust duct. The air moves from the inlet duct horizontally across the grain mass to the exhaust duct where it is vented to the atmosphere. A cooling front is established around the edge of the air inlet duct and "moves" through the grain with a velocity and shape that depends on air velocity and the geometry of the bin. This is the type of aeration cooling system studied in the research reported herein.

No relatively simple method of determining the progress of the cooling front has been presented to date. Most of the research which has been done on deep-bed aeration has been limited to linear air flow. Agricultural aeration facilities generally operate under non-linear flow conditions. Non-linear flow differs from linear flow in that the flow lines are divergent or convergent as opposed to being parallel as in linear flow. The mathematical analysis of deep-bed aeration is different for each geometric system and is formidable in any case.

The purpose of the current research was to develop a method of predicting the progress of the cooling front in the grain mass with any duct arrangement. An analogous, hydrodynamic, physical system called a fluid mapper was used to predict the position and shape of the cooling front at any time after the aeration process had begun (6).

TABLE 1—DEFINITION OF SYMBOLS

Symbol		Units
$A_b$	Cooled area of the cross-section of the test bin	$Ft^2$
$A_m$	Dyed area of the fluid mapper	$Ft^2$
$a$	Proportionality constant	— —
$a_m$	Proportionality constant	— —
$b$	Experimental constant	— —
$C_{pa}$	Specific heat of air	$\frac{BTU}{Lb-\text{°F}}$
$d$	Depth of flow space in the fluid mapper	$Ft$
$G$	Mass flow rate	$\frac{Lb}{Hr-Ft^2}$
$h$	Heat transfer coefficient	$\frac{BTU}{Hr-Ft^2-\text{°F}}$
$j_h$	Transfer function	— —
$k_a$	Thermal conductivity of air	$\frac{BTU}{Hr-Ft-\text{°F}}$
$l$	Any length in the test bin	$Ft$
$l_m$	Any length in the fluid mapper	$Ft$
$P$	Inlet duct pressure in the test bin	In. $H_2O$
$P_m$	Inlet duct pressure in the fluid mapper	In. $H_2O$
$\frac{\delta P}{\delta l}$	Partial of pressure with respect to distance in the bin	$\frac{In. H_2O}{Ft}$
$\left(\frac{\delta P}{\delta l}\right)_m$	Partial of pressure with respect to distance in the fluid mapper	$\frac{In. H_2O}{Ft}$
$Q_a$	Air flow rate	$\frac{Ft^3}{Hr-Ft}$
$Q_m$	Fluid flow rate in the fluid mapper	$\frac{Ft^3}{Hr-Ft}$
$R_n$	Reynolds number	— —
$T$	Temperature at any point in the test bin	$\text{°F}$
$T_a$	Original air temperature	$\text{°F}$

$T_o$	Original grain temperature	°F
TR	Temperature ratio $\frac{T-T_a}{T_o-T_a}$	-- --
$\alpha$	Scaling factor	-- --
$\beta$	Scaling factor	-- --
$\gamma$	Scaling factor	-- --
$\zeta$	Prediction factor	-- --
$\lambda$	Proportionality constant	-- --
$\mu_a$	Viscosity of air	$\frac{\text{Lb (mass)}}{\text{Hr-Ft}}$
$\mu_m$	Viscosity of fluid in the fluid mapper	$\frac{\text{Lb (force)-Hr}}{\text{Ft}^2}$
$\theta_a$	Time for the air to travel a given distance in the test bin	Hr
$\theta_c$	Time for the cooling front to advance a given distance in the test bin	Hr
$\theta_m$	Time for the dyed fluid to advance a given distance in the fluid mapper	Hr

### PREVIOUS APPROACHES TO POROUS MEDIA PROBLEMS

The phenomenon of heat transfer between a porous medium and a fluid flowing through the medium has been the subject of several investigations. As is true in most physical problems, three methods are generally available to be used in the solution of the problem. These methods are the analytic, graphical, and analogous approaches. The first provides an exact solution, the latter two generally provide approximations with varying degrees of accuracy.

*Analytic Approaches.* Schumann (14) developed a solution for the heating of a fluid by passing it through a porous bed of non-hygroscopic heated material. The problem was limited to one of sensible heat transfer and linear flow of the fluid. The results were presented as a family of dimensionless curves. The temperature of the fluid and the material could be predicted for any point in the

mass at any time after the process was started. Since the curves were based on dimensionless parameters, the solution presented was universally applicable to problems of this type.

Hukill (7) studied the problem of water vapor transfer from the porous mass to the air in the drying of agricultural products. He assumed the amount of heat necessary to evaporate the water was so much greater than the sensible heat transfer that the sensible heat could be omitted from the solution. Hukill's results were a family of dimensionless curves not unlike Schumann's results.

*Graphical Approaches.* Furnas (3) developed a method of obtaining the Schumann curves by graphical integration. Furnas also tested the Schumann analysis over a range of particle sizes and with several fluids. He concluded that the analysis was quite accurate.

Another method of obtaining the Schumann curves was developed by Ledoux (9). The method was a graphical integration which used the previous curve in the family of curves to obtain the next curve. Ledoux expanded the method to include non-uniform inlet air conditions and non-uniform original bed temperatures.

*Analog Approaches.* Many problems which have no apparent means of solution can be solved by analogy with some other physical system governed by the same conditions and equations. The problem of fluid flow in a porous medium is such a problem (8).

Botset (2) developed an analog to study the flow of fluid in the porous underground sand stratum. The analog was an electrolytic analog which operated on the principle that an ion in solution moves with a velocity proportional to the electrical gradient it is exposed to. This is analogous to the flow of fluid in the porous sand stratum. By use of the analog, Botset was able to determine the position of the oil-water interface during the flushing of oil bearing stratum. Muskat (12) showed that the analog gave adequate solutions.

Hele-Shaw (5) invented a fluid analog based on the theory that the flow of a viscous fluid in a restricted flow space is analogous to any field problem governed by Laplace's equation. In particular, it is analogous to the flow of an un-compressed fluid flowing in a porous medium. This analog device was called a fluid mapper and is the device used in this study of grain aeration cooling. The fluid mapper was later modified and refined by Moore (10, 11). He developed a solid dye front technique in which a dyed fluid was allowed to flow between two closely spaced plates to simulate an advancing front. One of the plates was glass so that the advance of the dyed fluid could be observed and photographed.

## EQUIPMENT

*The Fluid Mapper.* As mentioned previously, the basis of the fluid mapper is the flow of fluid between two closely spaced parallel plates. Physically, the fluid mapper consisted of an aluminum base plate with a recessed area machined into the surface (Figure 1). The recessed portion of the base plate was covered with a one-fourth inch glass plate, thus forming a flow space between the two plates. The recessed portion of the plate was the same shape as the grain mass being considered; in the case of the cylindrical grain tanks, it was circular. Two ports, representing the inlet and outlet air ducts of the prototype system, were located across the recessed portion of the base plate from each other. These ports extended through the base plate and were connected to supply tanks outside the water tray by one-eighth inch rubber tubing. A flow control valve was installed under the inlet port so that the flow of fluid over the surface could be started or stopped. The recessed area of the base plate was 12 inches in diameter. A one and one-half inch boundary around the recessed area was machined smooth to provide a sealing surface for the plate glass. When in operation, the plate glass was sealed to the base plate by stop-cock cement.

The entire fluid mapper was placed in a water-filled tray when in operation. This was to prevent air bubbles from being trapped under the glass plate as it was lowered onto the base plate. When the dyed fluid advanced through the flow space, it displaced the water already there.

*The Test Bin.* A test bin, the same shape as the recessed area of the fluid mapper, was constructed to check the predicted solution obtained from the fluid

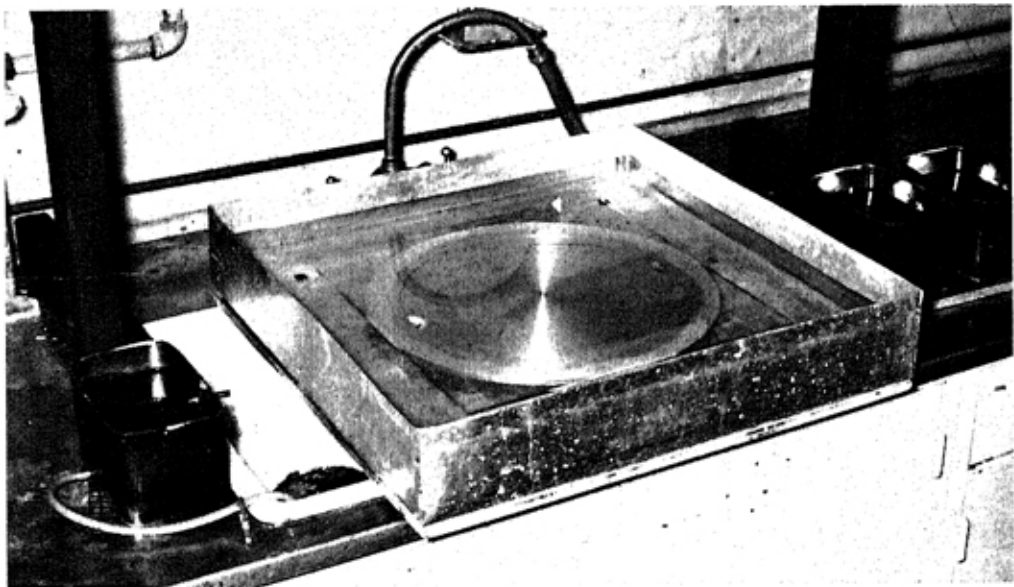


Fig. 1.—The fluid mapper with water tray, source tanks and glass plate in operating position.

mapper. The test bin was also used to provide experimental data for the evaluation of the proportionality constant between the analog and prototype systems. The bin and necessary control and recording equipment are pictured in Figure 2.

The bin was composed of three circular layers located so that a 6½ inch deep test layer was sandwiched between two 3¼-inch insulation layers. Each circular layer was 44 inches in diameter and the total capacity of the bin was 8.88 bushels. The inlet and outlet air ducts were located opposite each other on an axis of the test bin, and both extended through all three layers.

When the bin was in operation, all three layers were aerated. By this arrangement, a cooling front advanced through each of the insulation layers with approximately the same velocity as the cooling front in the test layer. Except for small errors introduced by heat loss from the insulation layers, the temperature patterns in all three layers were identical at all times. The similar temperature patterns prevented a significant temperature gradient between the test layer and the insulation layers, thus minimizing any heat loss from the test layer.

Each of the layers was equipped with a 3¼-inch by 4-inch tapered port to facilitate loading and unloading. These ports were located in the edge of each of the layers on an axis of the test layer perpendicular to the axis of the ducts. The entire bin was pivoted about the axis of the ducts to permit the bin to be loaded in the vertical position and operated in the horizontal position.

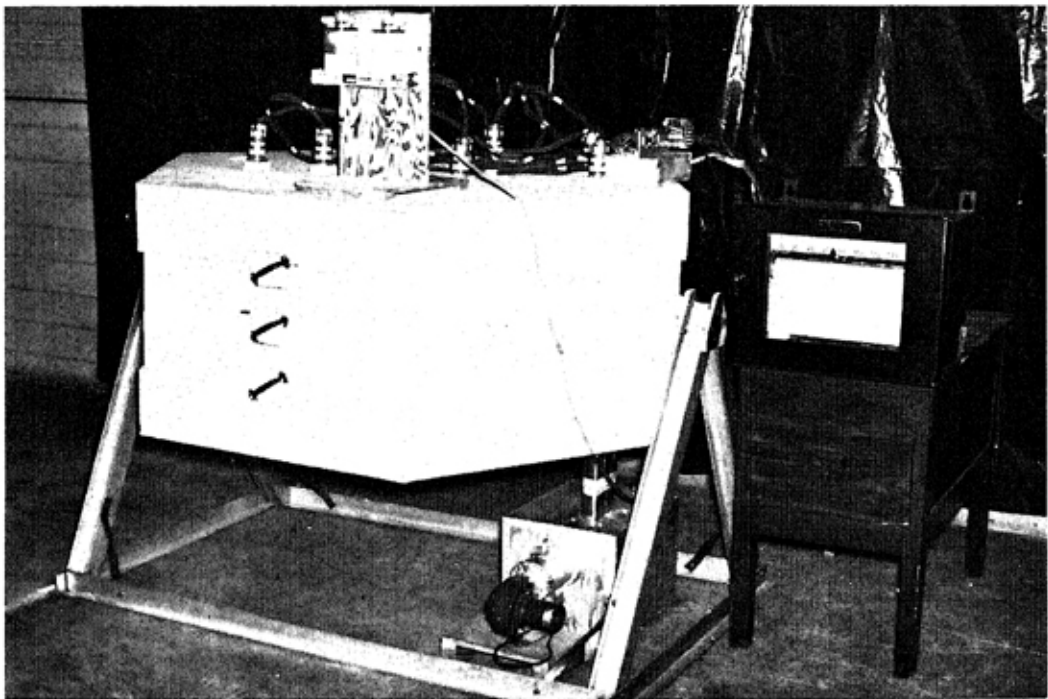


*Fig. 2—An over-all view of the experimental apparatus showing the fan, potentiometer, stepping switch and hook gage. The circular shaped test bin and insulation are located within the hexagonal shaped plywood shell.*



The temperatures of the grain mass were measured with 45 thermocouples located in the center of test layer. The thermocouples were imbedded in small sections of wooden dowel rods approximately the size of a wheat kernel. Thus, it was assumed that the thermocouples were reading an equivalent to internal grain temperature rather than air temperature.

The thermocouples were made of number 24 copper and constantan wire. After centering the junctions of the thermocouples in the small sections of dowel rod, the thermocouples were supported on one-fourth inch wooden dowel rods extending 3 inches into the test layer. The 45 thermocouples in the test layer were located on a 6-inch grid. Three thermocouples were located in the inlet duct.

The temperatures measured by the thermocouples in the test bin were recorded on a 16-point recording potentiometer. Since there was a total of 48 thermocouples (45 in the test layer and 3 in the inlet duct), the capacity of the 16-point potentiometer was exceeded. The capacity of the potentiometer was expanded by the use of a 25-point automatic electric stepping switch. The stepping switch operated on 110-volt alternating current and advanced one point each time a micro-switch was closed. The micro-switch was mounted on the potentiometer and was operated by the print crank. The thermocouple circuitry was similar to that described by Ohrenberg (13).

The thermocouple circuits were connected to the stepping switch from the test chamber by eight cannon connectors. This allowed the recording equipment to be disconnected from the bin when it was rotated into vertical position for loading and unloading.

Air was forced through the test bin by a small forward curved fan. The fan was connected to a 1 cubic foot plenum chamber which was, in turn, connected to the inlet duct of the bin. The amount of air being delivered to the bin was measured by the static pressure developed in the plenum chamber. The bin was calibrated by forcing a known amount of air through the filled bin and recording the static pressure developed. The air meter used for the calibration procedure was similar to the one described by Shedd (16). During calibration, the bin was filled with grain and the fan was removed. The duct was connected directly to the positive displacement air meter. The pressure developed by each of the flow rates which were to be tested, was read on a hook gage which was connected by one-eighth inch rubber tubing to the plenum chamber.

## TEST PROCEDURE

*Fluid Mapper.* The fluid mapper analog system was prepared for operation and operated by the following procedure:

1. The 1½-inch sealing boundary around the edge of the recessed area of the base plate was coated with stop-cock cement and the base plate was lowered into the water-filled tray.

2. The inlet and outlet fluid ports were connected to their supply tanks by means of rubber hoses passing through the bottom of the tray.

3. The water level in the tray and tanks was allowed to equalize and the water in the inlet supply tank was dyed with potassium permanganate crystals.

4. The plate glass used to cover the flow space was lowered onto the base plate and sealed in place by stop-cock cement so a water-tight seal completely surrounded the recessed flow space.

5. The inlet source tank was elevated one-half inch and the slide valve below the inlet port was opened.

6. A stop watch was placed at the edge of the test surface and the advancing dye front and watch were photographed every few seconds until the entire recessed flow space was filled with dyed fluid.

As the dyed fluid entered the flow space, a line between the dyed and undyed fluid moved across the fluid mapper surface. The line was analogous to the cooling front in the prototype grain bin of the same shape. Approximately two minutes were required for the dye to cross the fluid mapper surface when operated with a one-half inch hydraulic head. The data were obtained from the analog system in the form of the pictures taken of the dye front.

*The Test Bin.* Tests were conducted in the bin at three air flow rates (0.28 cfm/bu., 0.50 cfm/bu., 0.75 cfm/bu.). All tests were conducted in a chamber of the University of Missouri climatic laboratory where control was maintained over the inlet air temperature and relative humidity. The inlet air temperature varied less than plus or minus one-half of a degree during a test with an average temperature of between 66.2 and 68.0°F for the various tests.

The relative humidity of the inlet air was measured continuously. Since the research was concerned with cooling of the grain only, and not drying, an attempt was made to prevent a change in the grain moisture content during a test. The relative humidity of the inlet air was held as near the equilibrium relative humidity of the original grain moisture content as possible. The relative humidity in the control chamber varied as much as plus or minus 3 percent of the desired value; therefore, slight changes in the moisture content of the grain were expected. All tests included in the results of this report had a change in grain moisture content of less than one-half of 1 percent.

The cooling front in the grain test bin was defined to be the isothermal line along which the grain temperature had been reduced by 90 percent of the possible temperature drop between the original grain temperature and the inlet air temperature. The location of the isothermal cooling front was plotted on a scaled cross-section drawing of the grain bin at 4-hour intervals for each test conducted.

Air and grain conditions for each test conducted are summarized in Table 2.

TABLE 2 - GRAIN AND AIR CONDITIONS

	Air Flow Rate 0.28 Cfm/Bu		Air Flow Rate 0.50 Cfm/Bu			Air Flow Rate 0.75 Cfm/Bu	
	Test 1	Test 2	Test 1	Test 2	Test 3	Test 1	Test 2
Orig. Grain Temp. (F)	88.6	90.3	82.1	84.1	87.5	88.6	89.4
Inlet Air Temp. (F)	68.0	67.0	67.2	66.5	66.2	67.5	67.5
Change in Grain Temp. (F)	22.4	23.3	14.9	17.6	21.3	21.1	21.9
Inlet Duct Press. (In. H <sub>2</sub> O)	.046	.046	.080	.080	.080	.120	.120
Orig. Grain Moist. (per cent wb.)	10.79	9.84	11.34	11.42	11.24	10.05	9.51
Final Grain Moist. (per cent wb.)	10.78	9.72	11.09	11.27	11.51	9.63	9.72
Change in Grain Moist. (per cent wb.)	-.01	-.12	-.25	-.15	+.27	-.42	+.21

### VALIDITY OF THE ANALOG

Shedd (15) has shown that air flow rate ( $Q_a$ ) in a grain mass is related to the pressure gradient by the expression

$$Q_a = a \left( \frac{\delta P}{\delta l} \right)^b \quad (1)$$

wherein  $b$  is a function of velocity.

Shedd found that for low air flow rates, the exponent  $b$  is unity; therefore, the flow rate is proportional to the pressure gradient. When the inlet duct pressure is small enough that the air may be considered to be uncompressed, and when the flow of air in the porous grain mass is directly proportional to the pressure gradient, the air flow can be shown to be governed by the Laplacian field equation.

$$\Delta^2 P = 0 \quad (2)$$

The derivation of the Laplacian equation from the conditions stated above is included in the Appendix.

It has been shown that any field flow problem can be resolved to three basic parameters: a potential energy parameter, a kinetic energy parameter, and a dissipative parameter. Since the fluid in the mapper is uncompressed, no potential parameter is involved. For flow of a fluid through a restricted flow space at low velocity, the kinetic energy parameter is far outweighed by the dissipative force of viscous friction. Since the Laplacian field equation is valid for fields governed by one parameter, it was assumed that the fluid mapper is governed by the Laplacian equation. By application of the conditions of a Laplacian field to the general Navier-Stokes fluid flow equation, an expression similar to Shedd's equation was found for the flow of fluid in the fluid mapper.

$$Q_m = a_m \left( \frac{\delta P}{\delta l} \right)_m = \frac{62.4d^3}{144\mu_m} \left( \frac{\delta P}{\delta l} \right)_m \quad (3)$$

The derivation of this expression is included in the Appendix.

Since the flow equations of both systems have identical forms, it is assumed that the fluid mapper is an analog at the grain bin under aeration conditions. With the system equations known for each system, various scaling factors were defined to relate variables in the grain bin to corresponding variables in the fluid mapper.

### SCALING THE ANALOG SYSTEM

The proportionality constant ( $a$ ) of equation 1 was determined experimentally by Shedd (15). The proportionality constant ( $a_m$ ) of equation 3 is known as a function of the fluid viscosity and depth of flow space. The first scaling factor was defined to be the ratio of the two proportionality constants.

$$\alpha = \frac{a}{a_m} \quad (4)$$

Similar scaling factors were defined for the inlet duct pressure and size of each system.

$$\beta = \frac{P}{P_m} \quad (5)$$

$$\gamma = \frac{l}{l_m} \quad (6)$$

From equations 4, 5, and 6 a prediction factor ( $\zeta$ ), relating flow in the fluid mapper to the flow of air in the grain bin, was calculated.

$$\zeta = \frac{Q_a}{Q_m} = \frac{a \left( \frac{\delta P}{\delta l} \right)}{a_m \left( \frac{\delta P}{\delta l} \right)_m} = \frac{\alpha a_m \beta \left( \frac{\delta P}{\delta l} \right)}{a_m \left( \frac{\delta P}{\delta l} \right)_m} = \frac{\alpha \beta}{\gamma} \quad (7)$$

Thus, the flow of air in the test bin can be expressed as a function of the flow of the fluid in the mapper by:

$$Q_a = \zeta Q_m = \frac{\alpha \beta}{\gamma} Q_m \quad (8)$$

The total flow into the fluid mapper in a given time was found by operating the fluid mapper for a length of time ( $\theta_m$ ). After this length of time, a certain area of the fluid mapper was covered with the colored dye. The area ( $A_m$ ) was equal to  $Q_m \theta_m$ . Since area is dimensionally equal to the square of length, an area of the bin corresponding geometrically to the colored area of the fluid mapper can be expressed by the equation.

$$A_b = \gamma^2 A_m \quad (9)$$

The time required for air in the bin to advance from the inlet duct to a line corresponding to the leading edge of the colored zone in the fluid mapper was calculated as follows:

$$\theta_a = \frac{A_b}{Q_a} = \frac{\gamma^2 A_m}{\frac{\alpha \beta}{\gamma} Q_m} = \frac{\gamma^2}{\frac{\alpha \beta}{\gamma}} = \frac{\theta_m \gamma^3}{\alpha \beta} \quad (10)$$

For the fluid mapper to be an analog of the cooling zone in the grain bin, the velocity of the advancing cooling front along a flow path must be proportional to the amount of air moving along the flow path. This would require the heat transfer coefficient between the grain and air to be a constant value.

Gamson *et al.* (4) have shown that the heat transfer coefficient ( $h$ ) is nearly independent of temperature and relative humidity over short ranges of these variables. They also found the heat transfer coefficient was a function of the

mass flow rate ( $G$ ) under certain conditions. They defined a Reynolds number (called a pseudo Reynolds number by the authors) to be:

$$R_n = \frac{GD_p}{\mu_a} \quad (11)$$

for  $R_n$  less than 40, a transfer function was defined as:

$$j_h = \frac{18.1}{R_n} \quad (12)$$

The heat transfer coefficient was found experimentally to be a function of the transfer function.

$$h = j_h \frac{C_{pa} G}{\left[ \frac{C_{pa} \mu_a}{k_a} \right]^{.66}} = \frac{18.1 C_{pa}}{D_p \mu_a \left[ \frac{C_{pa} \mu_a}{k_a} \right]^{.66}} \quad (13)$$

Thus, as shown by equation 13, the heat transfer coefficient is independent of the mass flow rate ( $G$ ) for values of the Reynolds number less than 40. The value of the Reynolds number was less than 40 in all tests reported herein. On the basis of the foregoing, the heat transfer coefficient was considered to be a constant and the time required for the cooling front to reach a given point in the test bin was proportional to the time for the air to travel from the inlet duct to the point in question.

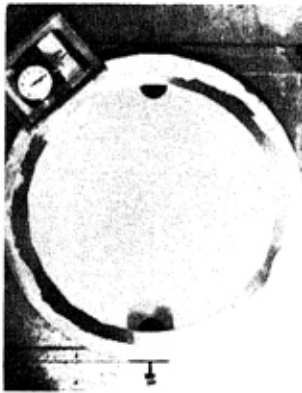
$$\theta_c = \lambda \theta_a = \frac{\lambda \gamma^3}{\alpha \beta} \theta_m \quad (14)$$

No analytic method of evaluating ( $\lambda$ ) was found. It was evaluated from experimental data using equation 14.

## DISCUSSION OF RESULTS

As explained previously, the data from the analog system were obtained by photographing the dye front on the surface of the fluid mapper at 5-second intervals. A sample of these time increment photographs is shown in Figure 3.

The results of the tests conducted in the experimental test bin are summarized in Table 3. The percent of the total cross-sectional area of the bin which had been cooled at a given time is recorded. A part of the data of Table 3 was converted to graphical plots showing the position of the cooling front in the test bin at various elapsed times. A composite drawing of these data from a representative test of each air-flow rate is shown in Figures 4, 5, and 6. The data from the test bin presented in this manner can be compared directly with the photographed results from the fluid mapper. The fluid mapper solution (Figure 3) appears, in general, to agree with the shape of the composite graphs of the cooling front shown in Figures 4, 5, and 6. The time for the cooling front to reach a given point in the test layer varied with the air flow rate; however, the shape of the cooling front at any given position is nearly the same for all air-flow rates.



TIME- 3.5 SEC.



TIME- 18.6 SEC.



TIME- 38.6 SEC.



TIME- 58.5 SEC.



TIME- 78.4 SEC.



TIME- 128.4 SEC.

*Fig. 3—Time increment photographs of the advancing dye front in the fluid map-  
per.*

TABLE 3 - PERCENT OF TOTAL CROSS-SECTIONAL AREA COOLED TO TR&lt;.1

Elapsed Time (hours)	Air Flow Rate 0.28 Cfm/Bu		Air Flow Rate 0.50 Cfm/Bu			Air Flow Rate 0.75 Cfm/Bu	
	Test 1	Test 2	Test 1	Test 2	Test 3	Test 1	Test 2
4	1.84	1.88	5.70	3.98	4.14	7.75	7.05
8	6.24	5.00	13.2	11.7	11.3	19.3	14.9
12	10.5	10.5	23.1	21.8	18.7	30.4	25.0
16	14.92	16.7	32.9	29.1	30.7	41.8	36.4
20		20.2	43.2	*	40.0	58.0	52.9
24	25.5	24.2	53.9	*	51.5	69.8	68.7
28		29.6	61.0	*	62.4	84.9	78.9
32	36.4	34.8	68.7	*	73.1	95.3	90.4
36		43.2	80.4	*	81.0		
40	48.1	50.2	86.4	*	89.5		
44		57.4					
48	62.6	65.0					
52		72.7					
54	78.5						
56		84.2					
58	91.4						
60		93.2					

\* Test terminated due to equipment failure



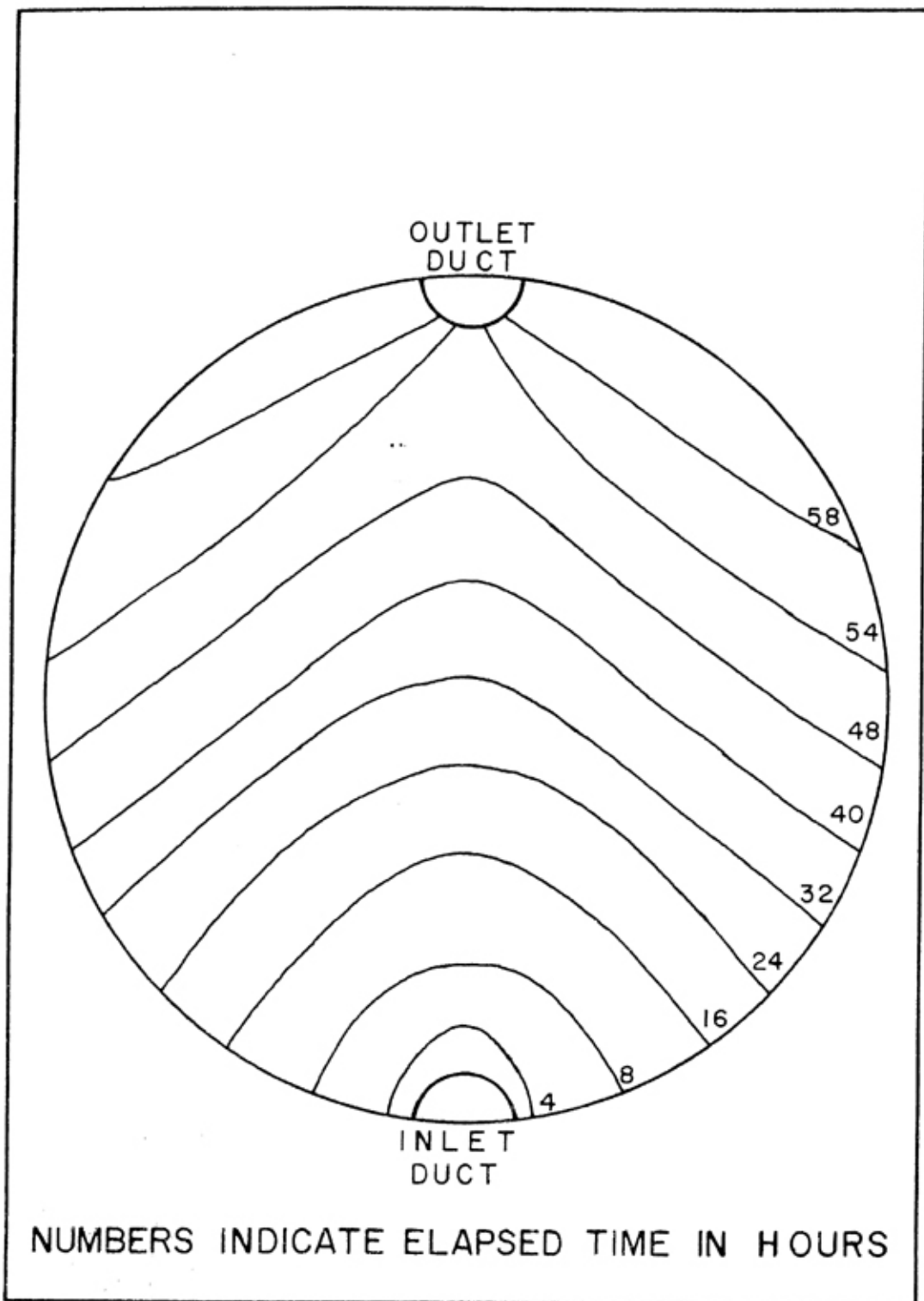
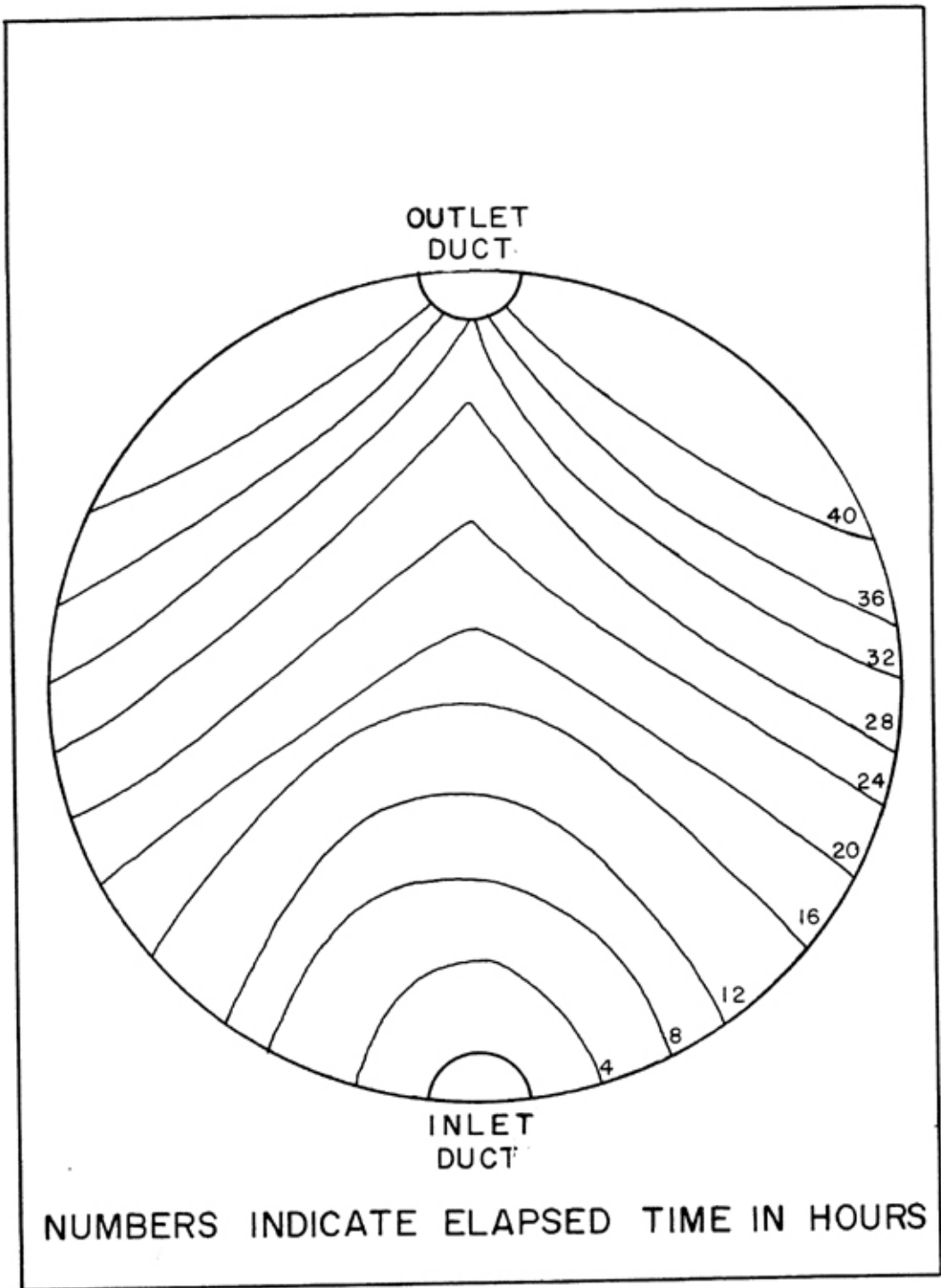


Fig. 4—A composite drawing of the advancing cooling front in the test bin in a representative test of air flow rate 0.28 Cfm/Bu.



*Fig. 5—A composite drawing of the advancing cooling front in the test bin in a representative test of air flow rate of 0.50 Cfm/Bu.*

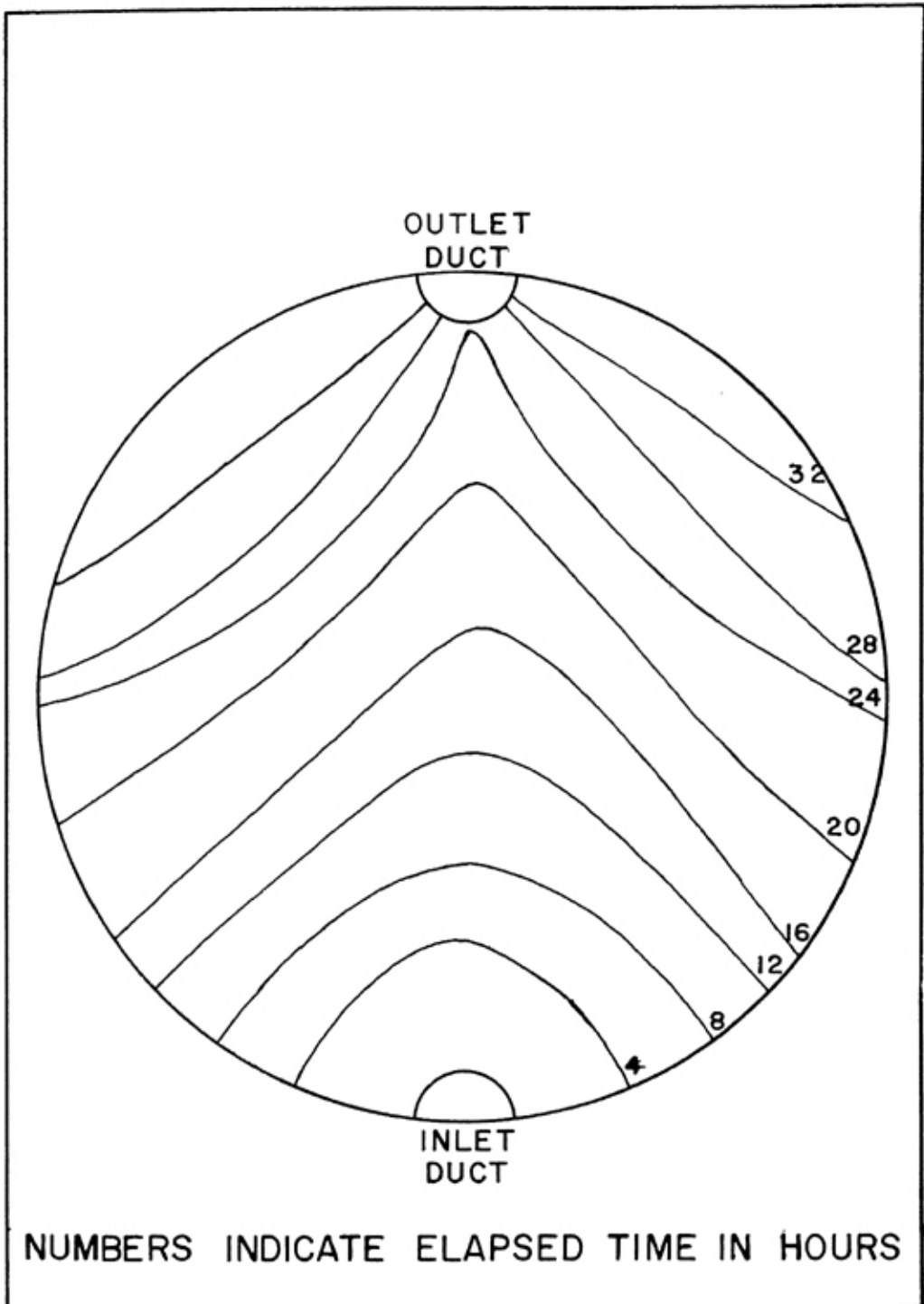


Fig. 6—A composite drawing of the advancing cooling front in the test bin in a representative test of air flow rate 0.75 Cfm/Bu.

The analog solution deviated from the experimental results near the edge of the flow space where viscous fluid friction against the wall caused the dye front to be held back. Since the boundary layer, caused by the friction, was quite evident and rather narrow, it created no serious difficulty in determining the position the dye front would have had with no boundary layer effect.

In Figure 7, the percent of total cross-sectional area of the bin that had been cooled was plotted against the elapsed time. No cool air escaped from the exit duct until approximately 65 percent of the bin had been cooled; therefore, a linear relationship between the area cooled and the time elapsed was expected. All of the data up to the time 65 percent of the total area was cooled were fitted with a linear curve by the method of least squares. The calculated lines are plotted for each air-flow rate in Figure 7.

To test the hypothesis that the cooling rate was proportional to the air-flow rate, the predicted cooling rates for the higher and lower air flow rates were calculated using the data from the tests with an air-flow of 0.50 cfm/bu. These predicted cooling rates are compared to the linear curves of the experimental cooling rates in Figure 8. The tests with an air-flow rate of 0.28 cfm/bu compared favorably with the 0.50 cfm/bu tests. The highest air-flow tests cooled more slowly than was predicted from the 0.50 cfm/bu tests. This discrepancy cannot be accounted for by the assumption that the heat transfer coefficient was not the same as in the tests with the lower air-flow rates, since a higher air-flow rate would cause a larger heat transfer coefficient and a faster cooling rate rather than a slower rate.

Difficulty was experienced in maintaining the required static pressure in the plenum chamber during the tests at the high air-flow rate. The static pressure gradually decreased and had to be corrected to its proper value from time to time during the test. Thus, during a part of each test at the highest air flow rate, the bin was not receiving as much air as it was calculated to receive. It was assumed that the decreased air flow rate caused the slower cooling rate.

The proportionality coefficient ( $\lambda$ ) between the test bin and the fluid mapper was calculated at 45 thermocouple positions in each of six tests. Due to the unstable inlet air-flow rate in the tests with the highest air-flow rate, these tests were not included in the analysis of variance. With these treatments removed, the remaining data consisted of two treatments, with two replications per treatment and 45 samples in each replication.

A summary of the statistical analysis of the variance of the proportionality coefficient data is shown in Table 4. The variance due to treatments (air-flow rates), replications, sampling error, and experimental error were removed from the total variance. The statistical F test was used to test the hypothesis that the experimental values of ( $\lambda$ ) were different for different treatments. The null hypothesis was that the experimental values of ( $\lambda$ ) were not significantly different for all air flows. The original hypothesis was rejected and the null hypothesis was accepted. Thus, it was assumed that the proportionality coefficient had, in fact, a constant value. The constant was evaluated from the mean of 180 estimates

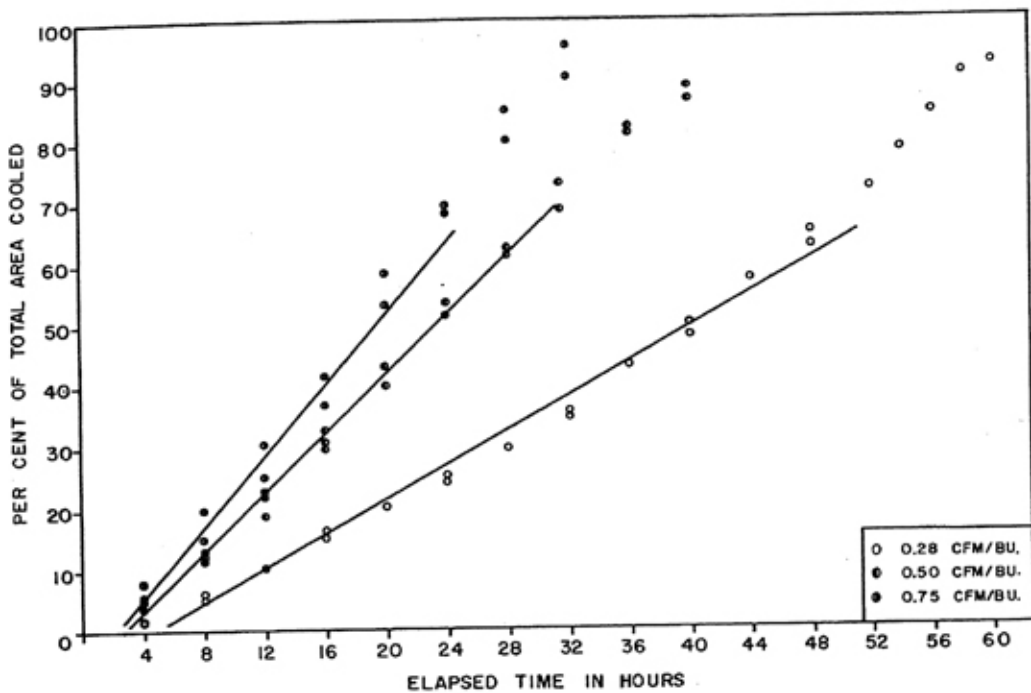


Fig. 7—Cooling rate curves for each air flow rate expressed as percent of total area cooled.

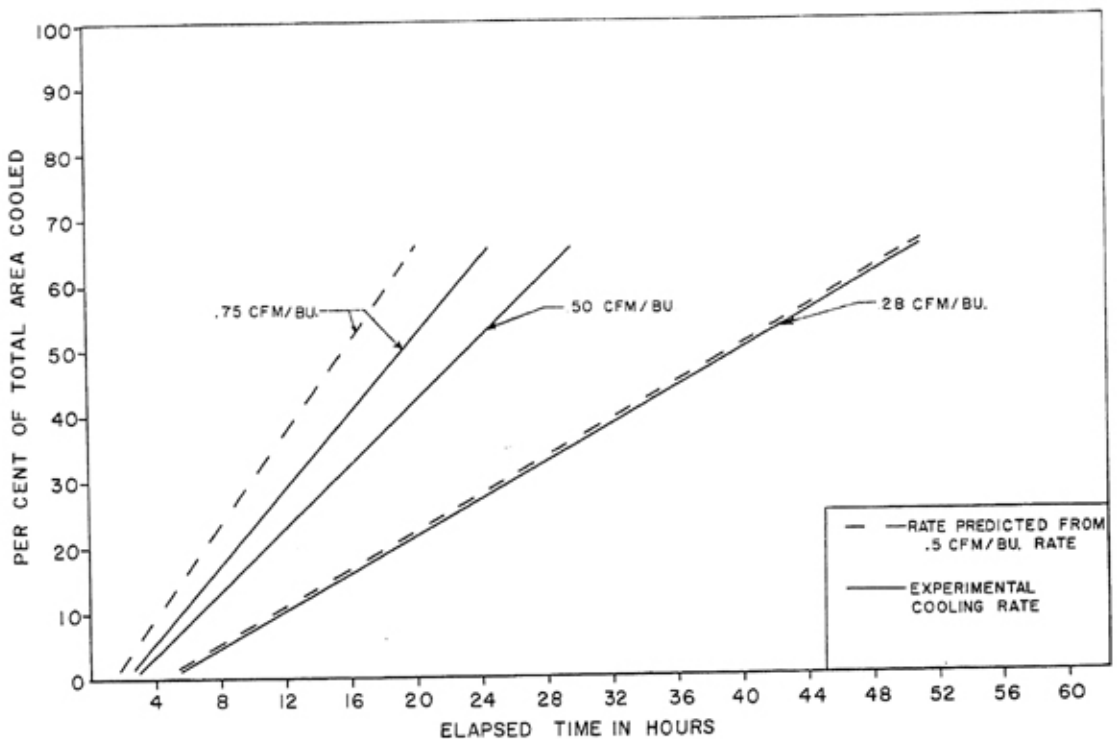


Fig. 8—Predicted cooling rate curves compared to experimental cooling rates. The predicted rates were calculated from the data of the tests with a 0.50 Cfm/Bu air flow rate.

TABLE 4 - ANALYSIS OF VARIANCE OF THE PROPORTIONALITY CONSTANT ( $\lambda$ )  
Based on air flow rates of 0.28 and 0.50 Cfm per bu.

Source of Variation	Sum of Squares	Degrees of Freedom	Mean Squares	F-Values	
				Calculated	50 Percent
Total	40,205,140	179	--	--	--
Treatments (flow rates)	15,493	1	15,493	.012	1.00
Replications	294,892	1	294,892	.228	1.00
Experimental Error	1,294,999	1	1,294,999	--	--
Sampling Error	38,910,141	176	221,080	.171	2.19

of the value and found to be 1500 for hard red winter wheat when less than one-half of one percent change in the moisture content occurred during the cooling process.

The proportionality coefficient *is independent* of the size or shape of the bin or fluid mapper or the amount of bin inlet duct pressure, provided the duct pressure is low enough to allow the pressure field to be a Laplacian field. The coefficient ( $\lambda$ ) *is* a function of the various parameters of the grain since the parameters are not included in the scaling factors. The grain parameters include resistance of the grain to air flow, heat transfer parameters of the grain, and the amount of moisture change in the grain during the cooling operation. Thus, the coefficient ( $\lambda$ ) would be expected to vary with the type of grain and amount of moisture change during a test.

The experimental and predicted cooling-rate curves are plotted in Figure 9. These curves were used only for comparison of the shape of the experimental and predicted cooling curves and not as a judgment as to the accuracy of the analog system, since the proportionality constant between the fluid mapper and the test bin was calculated from these same data.

Notwithstanding this limitation, significant differences and similarities between the analog and test results were noticed. First, the analog predicted a reduced cooling rate as the bin neared complete cooling. This was expected, as mentioned before, because of loss of dyed fluid or cooled air from the exit duct before the entire circle had been covered. The test bin showed this trend to varying degrees, but not to the extent that was predicted; and the lowest air-flow rate showed the opposite trend. These discrepancies may be explained by the fact that heat was being lost through the insulated walls of the test bin throughout the time a test was in operation. This caused the test bin to appear to cool faster near the end of a test than it actually should have. The effect of the heat loss was greatest in the low air flow tests because they took longest to complete.

The analog predicted solution and the experimental cooling-rate curves are both linear in the region between zero and 65 percent cooled. This was as expected since there was a constant fluid input to both systems with no loss until the cooled air or colored dye started to escape from the exit duct when approximately 65 percent of the area was either cooled or dyed.

Lastly, the two solutions differed in the fact that the analog solution shows no time delay before a portion of the area is covered, whereas, the experimental results indicate a delay. This is the reason the cooling-rate curves of Figure 7 do not pass through the origin. This difference was caused by the amount of time required to cool the first small volume of grain near the inlet duct to the temperature of the defined cooling front. This required cooling of the grain through 90 percent of the temperature difference between the original grain temperature and the inlet air temperature.

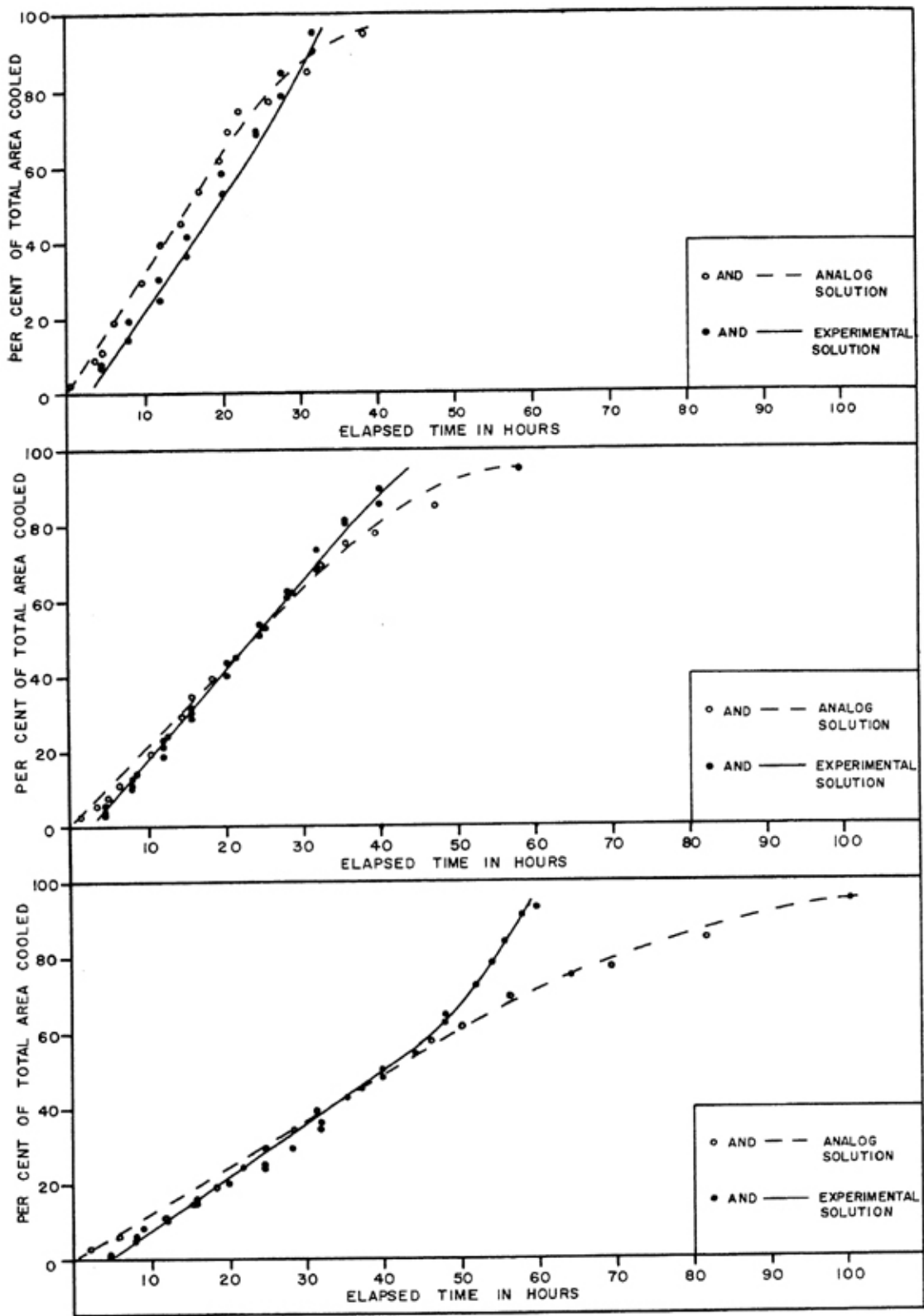


Fig. 9—Cooling rate curves predicted from the mean value of  $(\lambda)$  compared to experimental cooling rates.



## CONCLUSIONS

From this study, it was possible to conclude that the fluid mapper analog is a reasonably accurate device for predicting the progress of the cooling front in a grain mass in which the air flow can be represented in two dimensions.

The accuracy of the analog is dependent upon the extent to which the prototype system deviates from the Laplacian field. For the duct pressures and flow rates normally used in the grain aeration facilities, the analog is quite accurate.

The data reported in this investigation were limited to tests with little or no grain moisture change. The proportionality coefficient ( $\lambda$ ) was found to have a constant value of 1500 for hard red winter wheat with less than one-half of one percent change in grain moisture during the aeration process.

## BIBLIOGRAPHY

1. Agricultural Marketing Service. *Aeration of Grain in Commercial Storages*, Marketing Research Report No. 178, United States Department of Agriculture, Washington, Government Printing Office, 1960.
2. Botset, Holbrook G. "The Electrolytic Model and Its Application to the Study of Recovery Problems," *American Institute of Mining and Metallurgical Engineers*, Vol. 165 (1946), pp. 1-25.
3. Furnas, C. C. "Heat Transfer From a Gas Stream to a Bed of Broken Solids," *American Institute of Chemical Engineers*, Vol. 24 (1930), pp. 142-193.
4. Gamson, B. W., O. A. Hougen, C. Thodos. "Heat, Mass and Momentum Transfer in the Flow of Gases Through Granular Solids," *American Institute of Chemical Engineers*, Vol. 39 (1943), pp. 1-35.
5. Hele-Shaw, H. S., A. Hay, P. H. Powell, "Hydrodynamical and Electromagnetic Investigations Regarding the Magnetic Flux Distribution in Toothed-Core Armatures," *Journal of the Institute of Electrical Engineers*, Vol. 34 (1904-05), pp. 21-53.
6. Hohner, G. A. "Hydrodynamic Analog of Grain Cooling by Aeration," Unpublished Master's Thesis, The University of Missouri, 1964.
7. Hukill, W. V. "Basic Principles in Drying Corn and Grain Sorghum," *Agricultural Engineering*, Vol. 28 (1947), pp. 335-340.
8. Karplus, W. U., *Analog Simulation of Field Problems*. New York: McGraw-Hill Book Company, Inc., 1958.
9. Ledoux, Edward. "Dynamic Cooling of Adsorbent Beds," *Industrial Engineering Chemistry*, Vol. 40 (1948), pp. 1970-1977.
10. Moore A. D. "Fields From Fluid Mappers," *Journal of Applied Physics*, Vol. 20 (1949), pp. 790-804.
11. Moore A. D. "Further Development of Fluid Mappers," *Transactions of the American Institute of Electrical Engineers*, Part II, Vol. 69 (1950), pp. 1615-1624.
12. Muskat, M. *Physical Principles of Oil Production*. New York: McGraw-Hill Book Company, Inc., 1949.
13. Ohrenberg, A. J. "Use of Supplemental Heat in Corn Drying," Unpublished Master's Thesis, The University of Missouri, 1960.
14. Schumann, T. E. W. "Heat Transfer: A Liquid Flowing Through a Porous Prism," *Journal of The Franklin Institute*, Vol. 208 (1929), pp. 405-412.
15. Shedd, Claude K. "Resistance of Grains and Seeds to Air Flow," *Agricultural Engineering*, Vol. 34 (1953), pp. 616-619.
16. Shedd, Claude K. "Some New Data on Resistance of Grains to Air Flows," *Agricultural Engineering*, Vol. 32 (1951), p. 493.

## APPENDIX

DERIVATION OF THE LAPLACIAN FIELD EQUATION  
FROM THE NAVIER-STOKES FLUID  
FLOW EQUATION

For an incompressible fluid the Navier-Stokes fluid flow equations in Cartesian coordinates are:

$$\frac{\delta V_x}{\delta t} + \frac{\delta V_x}{\delta X} V_x + \frac{\delta V_x}{\delta Y} V_y + \frac{\delta V_x}{\delta Z} V_z = -\frac{1}{\rho} \frac{\delta P}{\delta X} + \frac{\mu_m}{\rho} \Delta^2 V_x$$

$$\frac{\delta V_y}{\delta t} + \frac{\delta V_y}{\delta X} V_x + \frac{\delta V_y}{\delta Y} V_y + \frac{\delta V_y}{\delta Z} V_z = -\frac{1}{\rho} \frac{\delta P}{\delta Y} + \frac{\mu_m}{\rho} \Delta^2 V_y$$

$$\frac{\delta V_z}{\delta t} + \frac{\delta V_z}{\delta X} V_x + \frac{\delta V_z}{\delta Y} V_y + \frac{\delta V_z}{\delta Z} V_z = -\frac{1}{\rho} \frac{\delta P}{\delta Z} + \frac{\mu_m}{\rho} \Delta^2 V_z$$

These general equations are limited by the following assumptions:

1. Assume steady flow, therefore,

$$\frac{\delta V_x}{\delta t} = \frac{\delta V_y}{\delta t} = \frac{\delta V_z}{\delta t} = 0$$

2. Assume laminar flow, therefore,

$$V_z = 0$$

3. Let  $V_{ave}$  equal average velocity and let  $R_n = \frac{V_{ave} \rho d}{\mu_m}$ . Reynolds number,

must be less than 1000 for the condition of laminar flow, therefore,

$V_{ave}$  must be small

$d$  must be small

$\mu_m$  must be large

4. For small  $V_{ave}$ ,  $\frac{\delta V_x}{\delta X}$ ,  $\frac{\delta V_x}{\delta Y}$  and  $\frac{\delta V_y}{\delta X}$ ,  $\frac{\delta V_y}{\delta Y}$  must be small compared to  $\frac{\delta V_x}{\delta Z}$

and  $\frac{\delta V_y}{\delta Z}$ .

Consider the term:

$$\frac{\mu_m}{\rho} \Delta^2 V_x = \frac{\mu_m}{\rho} \left[ \frac{\delta^2 V_x}{\delta X^2} + \frac{\delta^2 V_x}{\delta Y^2} + \frac{\delta^2 V_x}{\delta Z^2} \right] = \frac{\mu_m}{\rho} \frac{\delta^2 V_x}{\delta Z^2}$$

and likewise

$$\frac{\mu_m}{\rho} \Delta^2 V_y = \frac{\mu_m}{\rho} \frac{\delta^2 V_y}{\delta Z^2}$$

The preceding four relationships are substituted back into the original equations.

$$\frac{\delta V_x V_x}{\delta X} + \frac{\delta V_x V_y}{\delta Y} = -\frac{1}{\rho} \frac{\delta P}{\delta X} + \frac{\mu_m}{\rho} \frac{\delta^2 V_x}{\delta Z^2}$$

$$\frac{\delta V_y V_x}{\delta X} + \frac{\delta V_y V_y}{\delta Y} = -\frac{1}{\rho} \frac{\delta P}{\delta Y} + \frac{\mu_m}{\rho} \frac{\delta^2 V_y}{\delta Z^2}$$

$$0 = -\frac{1}{\rho} \frac{\delta P}{\delta Z}$$

The above equations are solved for the partial derivative of the pressure in each case.

$$\frac{\delta P}{\delta X} = \rho \left[ \frac{\mu_m}{\rho} \frac{\delta^2 V_x}{\delta Z^2} - \frac{\delta V_x V_y}{\delta Y} - \frac{\delta V_x V_x}{\delta X} \right]$$

$$\frac{\delta P}{\delta Y} = \rho \left[ \frac{\mu_m}{\rho} \frac{\delta^2 V_y}{\delta Z^2} - \frac{\delta V_y V_y}{\delta Y} - \frac{\delta V_y V_x}{\delta X} \right]$$

$$\frac{\delta P}{\delta Z} = 0$$

The three equations are differentiated again. The second derivative with respect to  $x$  and  $y$  of all velocity terms is assumed to be very small and is omitted.

$$\frac{\delta^2 P}{\delta X^2} = \mu_m \frac{\delta^3 V_x}{\delta Z^3} = 0; \quad \frac{\delta^2 P}{\delta Y^2} = \mu_m \frac{\delta^3 V_y}{\delta Z^3} = 0; \quad \frac{\delta^2 P}{\delta Z^2} = 0$$

Therefore,

$$\frac{\delta^2 P}{\delta X^2} + \frac{\delta^2 P}{\delta Y^2} + \frac{\delta^2 P}{\delta Z^2} = \Delta^2 P = 0 \quad \text{Laplace's Equation.}$$

## DERIVATION OF THE RESISTANCE TO FLUID FLOW IN A LAPLACIAN FIELD IN THE FLUID MAPPER

Consider the simplified Navier-Stokes equations obtained in the derivation for the Laplacian equation:

$$\frac{\delta P}{\delta X} = \mu_m \frac{\delta^2 V_x}{\delta Z^2}$$

$$\frac{\delta P}{\delta Y} = \mu_m \frac{\delta^2 V_y}{\delta Z^2}$$

$$\frac{\delta P}{\delta Z} = 0$$

Integrate with respect to Z:

$$Z \frac{\delta P}{\delta X} = \mu_m \frac{\delta V_x}{\delta Z} + C_1$$

$$Z \frac{\delta P}{\delta Y} = \mu_m \frac{\delta V_y}{\delta Z} + C_2$$

The boundary conditions are:

$$Z = 0 \quad \frac{\delta V_x}{\delta Z} = 0 \quad \frac{\delta V_y}{\delta Z} = 0$$

$$C_1 = C_2 = 0$$

Integrate again:

$$\frac{Z^2}{2} \frac{\delta P}{\delta X} = \mu_m V_x + C_3$$

$$\frac{Z^2}{2} \frac{\delta P}{\delta Y} = \mu_m V_y + C_4$$

The boundary conditions are:

$$Z = \frac{d}{2} \quad V_x = V_y = 0$$

$$C_3 = \frac{d^2}{8} \frac{\delta P}{\delta X} \quad C_4 = \frac{d^2}{8} \frac{\delta P}{\delta Y}$$

Substitute back into the previous equations.

$$\frac{Z^2}{2} \frac{\delta P}{\delta X} = \mu_m V_x + \frac{d^2}{8} \frac{\delta P}{\delta X}$$

$$\frac{Z^2}{2} \frac{\delta P}{\delta Y} = \mu_m V_y + \frac{d^2}{8} \frac{\delta P}{\delta Y}$$

Solve for  $V_x$  and  $V_y$ .

$$V_x = \frac{1}{2\mu_m} \left[ Z^2 - \left( \frac{d}{2} \right)^2 \right] \frac{\delta P}{\delta X}$$

$$V_y = \frac{1}{2\mu_m} \left[ Z^2 - \left( \frac{d}{2} \right)^2 \right] \frac{\delta P}{\delta Y}$$

The flow rate equals  $V_{ave}d$ .

$$Q_x = V_{ave}d = 2 \int_0^{\frac{d}{2}} V_x dZ = 2 \int_0^{\frac{d}{2}} \frac{1}{2\mu_m} \left[ Z^2 - \left( \frac{d}{2} \right)^2 \right] \frac{\delta P}{\delta X} dZ$$

$$= \frac{1}{\mu_m} \frac{\delta P}{\delta X} \left[ \frac{Z^3}{3} - \frac{d^2 Z}{4} \right]_0^{\frac{d}{2}} = - \frac{1}{\mu_m} \frac{d^3}{12} \frac{\delta P}{\delta X}$$

Therefore, flow in any direction

$$Q = - \frac{d^3}{12\mu_m} \frac{\delta P}{\delta l}$$

Therefore, the resistance to flow in the fluid mapper ( $a_m$ ) is equal to:

$$a_m = \frac{d^3}{12\mu_m}$$

When the pressure is measured in inches of  $H_2O$  the expression is changed to become

$$a_m = \frac{62.4d^3}{144\mu_m}$$